

Received March 26, 2021, accepted April 1, 2021, date of publication April 8, 2021, date of current version April 22, 2021.

Digital Object Identifier 10.1109/ACCESS.2021.3071796

A New Deep Stacked Architecture for Multi-Fault Machinery Identification With Imbalanced Samples

HANEN KARAMTI^{1,2}, MAHA M. A. LASHIN^{3,4}, FADWA M. ALROWAIS¹,
AND ABEER M. MAHMOUD⁵

¹Computer Sciences Department, College of Computer and Information Sciences, Princess Nourah bint Abdulrahman University, Riyadh 11564, Saudi Arabia

²MIRACL Laboratory, Higher Institute of Computer Science and Multimedia of Sfax (ISIMS), University of Sfax, Sfax 3029, Tunisia

³College of Engineering, Princess Nourah bint Abdulrahman University, Riyadh 11564, Saudi Arabia

⁴Mechanical Engineering Department, Faculty of Engineering Shoubra, Benha University, Banha 13518, Egypt

⁵Department of Computer Science, Faculty of Computer and Information Sciences, Ain Shams University, Cairo 11566, Egypt

Corresponding author: Fadwa M. Alrowais (fmalrowais@pnu.edu.sa)


This work was supported by the Deanship of Scientific Research, Princess Nourah bint Abdulrahman University, through the Program of Research Project Funding After Publication under Grant 41-PRFA-P-38.

ABSTRACT Effective intelligent fault diagnosis of rotating machinery using its vibrational signals has a considerable influence on certain analysis factors such as the reliability, performance, and productivity of a variety of modern manufacturing machines. Traditional intelligent approaches lack generalization schemes and add the burden of extracting features from data-driven cases. On the other hand, the Deep Learning (DL) studies have reported capabilities higher than the expectations of the researchers' objectives. In this context, this paper proposes a new deep architecture based on Stacked Variant Autoencoders for multi-fault machinery identification with imbalanced samples. The proposed model starts with a Variational Autoencoder (VAE) for facilitating data augmentation of small and imbalanced data samples using Gaussian distribution. After the preparation of suitable samples based on quality and size, the preprocessed vibration signals obtained are injected into the deep framework. The proposed deep architecture contains two subsequent unsupervised Sparse Autoencoders (SAE) with a penalty term that helps in acquiring more abstract and essential features as well as avoiding redundancy. The output of the second SAE is integrated on a supervised Logistic Regression (LR) with 10 classes. This is utilized for the proposed classifier training to achieve accurate fault identification. Experimental results show the efficiency of the proposed model which achieved an accuracy of 93.2%. In addition, for extensive comparative analysis issue, the Generative Adversarial Network (GAN) and triNetwork Generative Adversarial Network (tnGAN) were both implemented on the vibrational signal data, where the proposed method reported better results in terms of training and testing time and overall accuracy.

INDEX TERMS Fault diagnosis, imbalanced samples, logistic regression, rotating machinery, sparse autoencoders, variational autoencoder, vibrational signals.

I. INTRODUCTION

Defects in rotating machinery are considered a core challenge during the analysis of causes of low productivity for certain systems and applications. Generally, faulty gears lead to irregular performance of the machine, where different types of fault appear with different frequencies [1], [2]. The literature has shown that tackling such problems successfully

The associate editor coordinating the review of this manuscript and approving it for publication was Dazhong Ma .

requires two major phases: feature extraction of the produced signals and an intelligent classifier for the final diagnostic mission [3]–[6]. Existing research on diagnosing faults in rotating machinery can be divided into studies focusing on traditional artificial intelligence techniques that include fuzzy logic [7], [8], genetic algorithms [9], support vector machines [10] and neural networks [11] or more recently, deep learning artificial intelligence techniques [12], [13].

Researchers used traditional techniques for mainly small samples of available data and minimized time complexity;

however, they struggled with low efficiency and poor generalization characteristics. In such techniques, feature extraction is a necessary phase that consumes effort and time, with the possibility of not reaching optimality and affecting overall performance. Therefore, it is essential to apply (1) a reasonable data preprocessing method, (2) a suitable traditional algorithm, and (3) a heuristic algorithm for optimization. To solve this problem, Zair *et al.* [8] used the fuzzy entropy of empirical mode decomposition, Principal Component Analysis (PCA), and a self-organizing map type of neural network to diagnose rolling bearing faults. They first decomposed the vibration signals into a series of intrinsic mode functions to obtain the features. They then optimized the features with fuzzy entropy, reduced their dimensionality with PCA, and classified them with a self-organizing map neural network. Ramos *et al.* [7] designed a new data-driven based fault diagnosis system based on fuzzy clustering techniques. The authors preprocessed the data for feature extraction then used the Kernel Fuzzy C-means algorithm to differentiate classes of faults. Their model was validated on benchmark data sets and indicated the feasibility of this approach. Cerrada *et al.* [9] built a multi-stage feature selection approach for vibration signals for fault diagnosis in gearboxes. They used genetic algorithms, for optimization in multiple stages, combined with a neural network for classification. They reported levels of high accuracy in different running conditions of data parameters. Pan *et al.* [10] combined the wavelet-packet approach with PCA to accurately extract the important features. They then used the multiple kernel function with a fusion method in a support vector machine to classify the gear faults and reported high diagnostic accuracy. Mekki *et al.* [11] used an artificial neural network to estimate the output and detect faults of a photovoltaic module under certain conditions. They then compared the estimated results versus the ones measured. The authors showed the effectiveness of the proposed method, using several shading patterns and accurately detected module faults.

As an alternative to the traditional methods, deep learning techniques (DAs) [14]–[18] are recommended for more efficient and accurate results. However, large data samples are needed to avoid over-fitting, or flexible augmentation is needed to increase the number of samples for training deep frameworks, if possible. Zhu *et al.* [12] proposed a deep learning model based on a convolutional neural network (CNN) that can efficiently and accurately recognize vibration faults by automatically extracting rotor vibration features. They then diagnosed the faults and reported enhanced results compared to traditional methods. To diagnose rotating machinery faults. Guan *et al.* [13] devised a novel combination of empirical mode decomposition (EMD), sample entropy, and a deep belief network (DBN). This approach was validated on fault signals and their comparative experiments demonstrated superior performance using this method.

Using deep learning techniques reduces the burden of feature extraction, as it is achieved automatically and more

efficiently. The researchers in this study were inspired to attempt the advantages of a deep learning approach to solve the challenge of accurate fault diagnosis for rotating machines using vibration signals. Although a variety of modules have been proposed in the literature, most require certain constraints on preparing the signal input and the problem still highlights the need for a new framework that better fits the defined problem and needs fewer complex parameter adjustments.

This paper proposes a novel deep learning architecture for diagnosing rotating system faults using vibration signals. The proposed architecture is composed of a Variational Autoencoder (VAE), followed by two sparse autoencoders for feature extraction and elimination of unnecessary information, followed by a fully connected layer that corresponds to a Logistic Regression for fault classification.

The innovated contribution of this paper is proposing a new Deep Predictive Model architecture based on two types of autoencoders for signal diagnosing of multi-faults. The first Variational autoencoder was used for accomplishing the augmentation challenge and suitably enriching and preparing data for the deep model. The Sparse autoencoder was used to control the abstraction of the signals valuable features to reach an optimal performance. Another main contribution of this paper is the supporting that could be provided for several industries by using the proposed aided diagnostic system for easily identifying the machine faults, even if they do not have a great knowledge about machine utilization. In addition, we presented a comparative analysis for different classifiers motivated by solving identical issues. In addition, we conducted various experiments, as shown in this paper, to validate the proposed model.

The paper is organized as follows: Section II presents some recent related work. Section III provides a detailed understanding of the type of rotating machine included in this study and its main nomenclatures and possible types of faults, depicted in figures. The basic concepts and development status of the proposed methodology with a hierarchical structure for the deep framework are presented in Section IV. The computational tests, analysis, and discussion are accompanied by the required preprocessing information on the dataset used in Section V. The conclusion in Section VI summarizes the research and its contribution.

II. RELATED WORK

A variety of deep learning diagnostic models for rotating machines has been proposed in the literature. These models can be classified according to the type of neural architecture used in their building. Most traditional usage of neural networks is built based on PCA. However, it is known that PCA uses only forward learning and thus fails to solve nonlinear problems. Hence, the use of back-propagation increases the capability of neural network learning and generates different models. In addition, the number of hidden layers in the architecture represents a key difference between the existing models and consequently affects performance. Deep Learning

(DL) facilitates the automatic conversion of simple features into a complex and abstract version.

A fault diagnosis approach based on a wavelet transform scalogram and a Pythagorean spatial pyramid pooling CNN was proposed by Guo *et al.* [19]. The vibration signals are decomposed according to the spinning speed using the continuous wavelet transform. After that, the CNN receives the various signal sizes. To compare the findings, they used a spatial pyramid-pooling layer in the CNN. Accordingly, adding the spatial pyramid-pooling layer in the CNN reached a higher diagnostic accuracy. Hasan and Kim [20] converted features of the vibration signal in the form of images, then used conventional methods to classify the faults of bearings. The effectiveness of their approach was verified by the experimental data obtained. Huang *et al.* [21] designed a deep decoupling convolutional neural network for discriminative feature extraction from raw vibration signals. The authors then combined this design with multi-stack capsules as a classifier to accurately identify the faults. Finally, they used the routing-by-agreement algorithm for optimization. They validated their system by using gearbox fault tests and reported promising results from the designed model.

Zhang *et al.* [22] proposed a fault diagnosis model using raw sensor data and Deep Neural Networks (DNN) without feature selection or signal processing. They measured the classification accuracy after training their model until the cost feature was reduced. The proposed model had the greatest accuracy in distinguishing the various types of bearing faults. Yang *et al.* [23] suggested a deep learning model for clustering bearing signals automatically. First, they extracted the signals' frequency domain, then used the DNN to classify the signals. They showed that their model accurately achieved automatic clustering for the vibration of faulty signals. He *et al.* [24] developed a deep belief network (DBN) for unsupervised gear vibration fault diagnosis. They then used a genetic algorithm for optimization of the network parameters. The authors then compared their system with traditional artificial intelligence methods (back-propagation neural network and support vector machine) on the same dataset and demonstrated promising results for the deep learning model.

Jiang *et al.* [25] developed a stacked denoising autoencoder based on a multivariate data-driven fault detection framework. They also introduced a multilevel noising method to enrich the generalization of their model. They evaluated their proposed framework on both simulated data and real data and showed competitive levels of accuracy. Liu *et al.* [26] built a stacked autoencoder based on a deep learning model for solving early detection of gearbox faults from data-driven analysis. Their model directly extracts salient features from frequency-domain signals, which saves the effort of handcrafting features. They confirmed significant improvement using this method.

Generally, some neural network models, such as CNN, require converting the raw signals into image data, whatever the approach used (e.g., wavelets transform, acceleration-time series, etc.). Some other models, such as deep belief

networks, require a longer time for training, more complex treatment for the input, and require a high probability to fall into local optima. However, the autoencoder can handle raw data more simply and precisely. Accordingly, based on the results reported in the previous research, the autoencoders, with their variety of functions, recorded the highest classification accuracy compared to Artificial Neural Network (ANN), CNN, and other deep learning models. Hence, the autoencoders advocated to use a different combination of architectures and nominated to participate in the deep learning frameworks intended for diagnosing faults of machinery infrastructures. The authors of this study were motivated by the information concluded from related work and propose an autoencoder-based framework to investigate the performance in case of imbalanced small samples of data from the rotating machine which that is described in the next section in this paper. The methodology section then details the contents of the proposed model.

In terms of not accurate data detection, the existing samples could not be considered as enough effective to train the model. To address this problem, generative models are proposed like the Generative Adversarial Networks (GANs) and the Variational Autoencoders (VAEs). For ensuring data reliability, Zhang *et al.* [27] proposed the mixedGANs model (mixed generative adversarial networks) to generate additional data by creating multitype generative networks including heterogeneous parameters. This solution provides several solutions and prevents the unexpected risks of unstable training.

Hu *et al.* [28] used the generative adversarial network applied on triNetworks (tnGan) to resolve the leak detection issues with incompleteness sensor data. The proposed tnGAN is employed to recuperate incomplete data by fully exploiting similar features on the same level. The input data were extracted from similar sensors, that were obtained from the pipeline network. Then, in order to facilitate the integration of inherent information, they integrated it into their model a multiview awareness strategy and in order to detect pipeline status, they proposed dual-discriminative network architecture.

Shao *et al.* [29], implemented a modified stacked autoencoder based on wavelet to diagnose different faults of rotating machinery. Firstly, they accomplished a nonlinear mapping between the raw vibration data and different fault states. Secondly, they enhanced the cost function towards enhancing the sparsity and the reconstruction results. In addition, an optimization was proposed for adjusting the parameters and enhancing the performance. The proposed method was validated on two types of mechanical units (sun gear and a roller bearing unit).

Hea *et al.* [30], targeted the treatment of few samples problem by proposing a deep transfer multi-wavelet auto-encoder. Firstly, they designed a new deep multi-wavelet auto-encoder for obtaining the most discriminative features from vibration signals of gearbox. Secondly, they selected the samples that were more similar to original samples for training. Finally,

the knowledge from training was transferred to target model using reduced set of samples. They proved reliability even with significant changes.

III. DESCRIPTION OF ROTATING MACHINE DEFECTS

To perform an intended operation, a mechanical machine employs power to apply forces and manipulate movement [31]. Additionally, any rotating machine device that rotates, is either a driving or driven system. Driving systems, such as electric motors, combustion engines, and generators convert rotational motion into translational motion and match between speed and torque, as achieved through a pulley, gearbox, and chain. As shown in Fig. 1, a complete rotating machine contains a motor (driver), coupling and gearbox (transmission speed device between driver and driven), and pump (the driven part in the machine) [32].

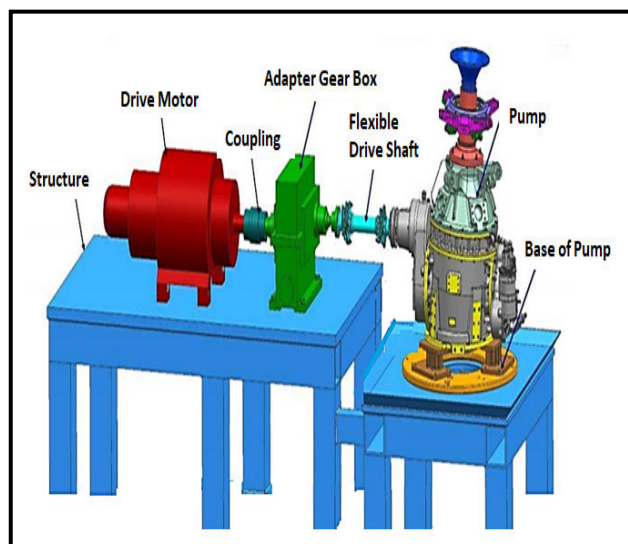


FIGURE 1. Complete rotating machine [32].

The most common defects in rotating machines can be summarized in ten types: motor defects, misalignment, gear defects, unbalance, resonance, mechanical looseness, structural looseness, soft foot defects, oil whirl, and bearing defects.

A. MOTOR DEFECTS

The spinning machine's driver, the electric motor, transforms electrical energy into mechanical energy, as shown in Fig. 2. (a, b). It generates a linear or rotary force (torque) that is intended for continuous rotation or linear movement over a large distance relative to its size. The main defects that can appear in electrical motor are a broken tooth on the sprocket and a broken rotor coil, as shown in Fig. 2 (c, d) [33], [34].

B. MISALIGNMENT

The machine coupling is the device used to connect two shafts of rotating machines together at their ends to transmit power, as shown in Fig. 3 (a and b). Misalignment in machine

coupling means eccentricity, where the axes or centerlines of two coupled shafts do not coincide with each other [35]. Parallel, angular, and combined misalignments are shown in Fig. 3 (c and d).

C. GEAR DEFECTS

Any rotating machine's gear system is primarily dependent on the gear. As shown in Fig. 4 (a and b) [36], the gear is a part with cut teeth, each of which meshes with another toothed part to transmit torque to adjust the speed, torque, and direction of a power source. The Most gear faults occur in the tooth surface, such as a pitted tooth, or in the breakage of the gear tooth such as a cracked, chipped, or missing tooth, as shown in Fig. 4 (c).

D. MACHINE UNBALANCE

A rotating machine is unbalanced (or out of balance) where there is an unequal distribution of mass, for example where the center of mass (inertial axis) is out of alignment with the center of rotation (geometric axis), which creates a centrifugal force, as shown in Fig. 5 (a and b) [37].

E. RESONANCE

Resonance occurs when the natural frequency of the machine is at or close to a forcing frequency coming from outside the machine. Resonance defects produce vibration that has a bad effect on the machine and on the whole structure [38].

F. MECHANICAL LOOSENESS

This fault appears when there is insufficient tightening between different mechanical elements. Loosening of machine bolts or fracturing of fixations are examples of this form of defect, which can lead to an increase in tolerances caused by wear and tear, as well as excessive gaps in rolling element bearings, sleeve bearings, and gears [39].

G. STRUCTURAL LOOSENESS

This fault refers to looseness in the machine's mechanical non-rotating parts, such as bench fixings, pipe joints, bearing casings, and so on. It usually manifests itself more clearly in the radial measurement directions than in the axial ones, with the frequency spectrum containing several harmonics of the shaft's rotating speed. When the amplitude of the $2\times$ and $3\times$ harmonics is compared to the frequency at $1\times$, the severity of looseness can be determined: If the amplitude of these harmonics reaches 50% of the amplitude of the peak at $1\times$, this happens. The explanation why this kind of looseness manifests in frequency spectra with many harmonics of the rotating frequency is shown in Fig. 6 [40] ($1\times$, $2\times$, $3\times$, $4\times$, etc.). Due to loosening of the fixings between the bearing supports and the seat, the motor poses a slight unbalance as the driving force of the looseness. As the unbalanced heavy spot rotates to complete a full revolution, we can see that there are four forces or impulses, two of which are due to the unbalance and the other two due to the return of each of the sides of the support to the bench, as seen in the four stages

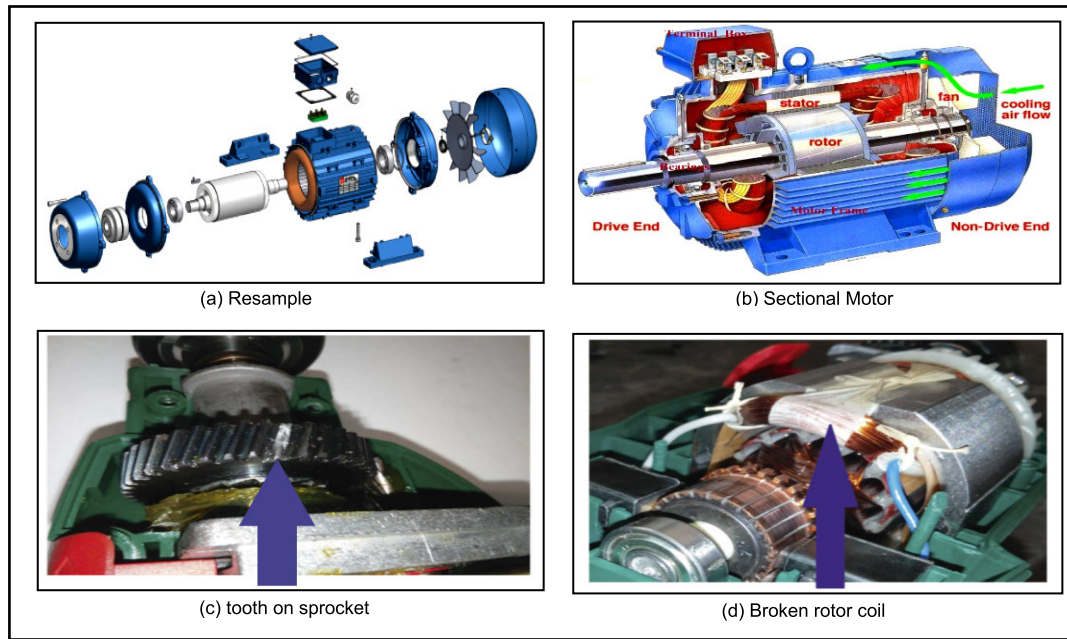


FIGURE 2. Electrical motor [33], [34].

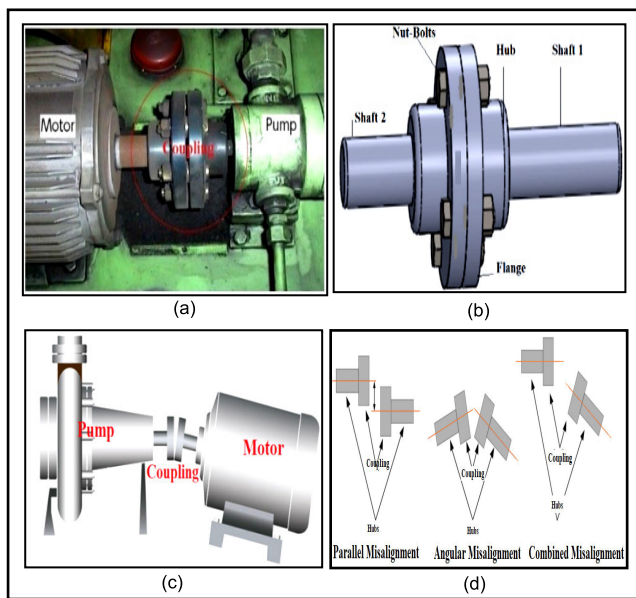


FIGURE 3. Coupling misalignment [35].

of Fig. 6. In the vibration spectrum, this can result in several harmonics of the spinning frequency.

H. SOFT FOOT DEFECT

The effects of soft foot on machinery alignment are even more harmful because it distorts and strains the machine’s frame. As shown in Fig. 7 [41], the shafts’ rotational centerlines will not be consistent, causing problems with coupling wear, rotor air gap, bearing/seal fit, and clearance issues. Lasers have made measuring misalignment simpler and easier since their launch.

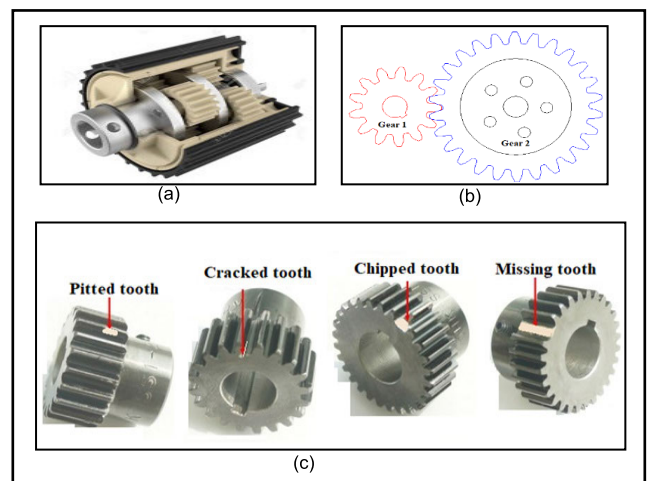


FIGURE 4. Gear system [36].

I. BEARING DEFECTS

Fig. 8 (a) explains the purpose of the bearing system of any rotating machine, as it is used for supporting the shafts of that machine. The main components of the bearing are the inner race, outer race, balls, and cage, as shown in Fig. 8 (b). Bearing defects can be seen in these parts, as shown in Fig. 8. (c). Bearing failures result in a variety of issues, including improper rotating machinery operation [42].

J. OIL WHIRL

This fault defines a form of subsynchronous vibration that travels at about half-speed until the speed reaches two times the first critical speed. The subsynchronous vibration

TABLE 1. Machine defects samples.

Motor defect	Rotating Machines Defects										
	Misalignment		Gear defect	Unbalance defect	Resonance defect	Mechanical looseness defect	Structural looseness defect	Soft foot defect	Bearing defect	Oil whirl	
M2DEAV	PMAV	PMHV	GB2HV	GBAV	BVBA	OWHV	MechLVV	PLAV	SFFVV	BGBAVDE	OWJ BHV
M2DEHV	PMISAV	PMISHV	GB3AV	GBDEAV	BVBV	SRHV		PLHA	SFFVV2	BGBHVDE	
M2DEVV	PMISVV	PMVV	GB3VV	GBDEHV				PLHV	SFFVV3	BGBVVDE	
MDEAV	P2MAV	P2MHV	GB4HV	GBDEVV					SFFVV4		
MDEHV	P2MVA	P3MAV	GB5AV	GBHA							
MDEVV	P3MHV	P3MVV	GB2VV	GBHV							
	GB4AV	GB3HV	GB4VV	GBVD							
	GB5HV	GB5VV	GBVV								

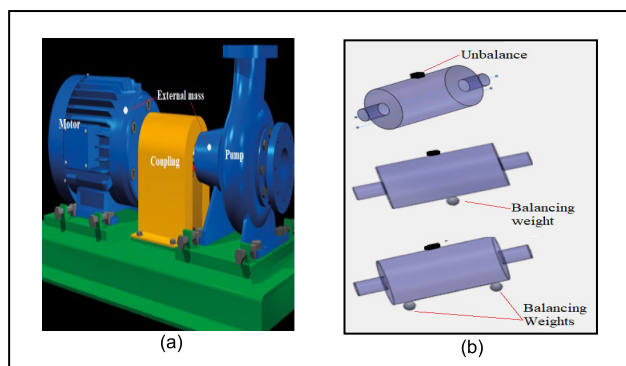


FIGURE 5. Machine with unbalance [37].

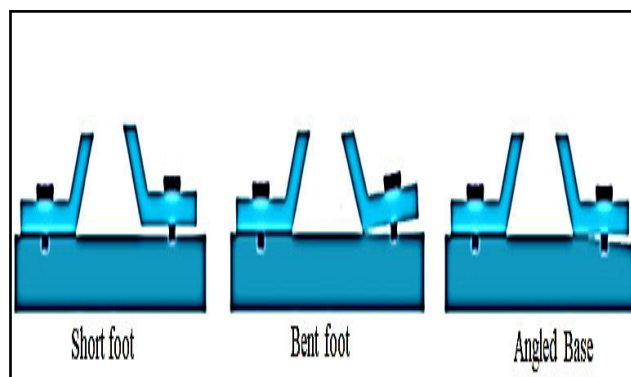


FIGURE 7. Soft foot defect [41].

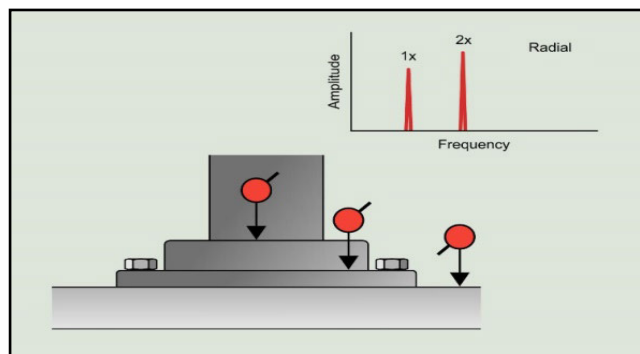


FIGURE 6. Structural looseness [40].

will remain near the first critical speed as the speed increases [43].

IV. DIAGNOSTIC METHODOLOGY

This section describes the proposed intelligent fault diagnosis model. First, the signals are extracted and preprocessed to extract the features. Since the collected data is inadequate for training, an augmentation phase is needed to produce additional signals from the original data. The variational autoencoder is used for this purpose. Following that, we suggest using two unsupervised sparse autoencoders to train the model with an emphasis on feature extraction, followed by a supervised LR to locate the fault. Finally, the proposed model is put to the test to see how effective it is. Fig. 9 represents the

proposed model and the flowchart presented in Fig. 10 details the steps taken to construct our system.

A. DATA COLLECTION

The data used in this research paper is real data obtained from a company that provides monitoring and maintenance services to factories and various industrial companies. Table 1 shows the different types of defects in machines that were discovered by using measuring devices that measure the mechanical vibrations generated by the machines during their operation and analyze them to determine the type of defects in the machines for treatment and repair later.

Researchers have used a variety of criteria to identify flaws. We gathered ten types of faults related to the machine type mentioned in section three, as stated in Table 1, for this analysis.

B. SIGNAL PREPROCESSING AND NORMALIZATION

Signal filtration, normalization, noise removal, and feature extraction are some of the preprocessing steps that are for data consistency and to minimize undesired time waste while training the model. These crucial measures lighten the autoencoder’s load and improve its efficiency in obtaining the most useful features. The data is sampled at 64 kSa/s for 4 seconds, while the shaft is rotated at 1200 or 900 rpm, which corresponds to 30 and 20 Hz, respectively.

The data used is insufficient to train the target model because it has a long time and a high frequency. To increase

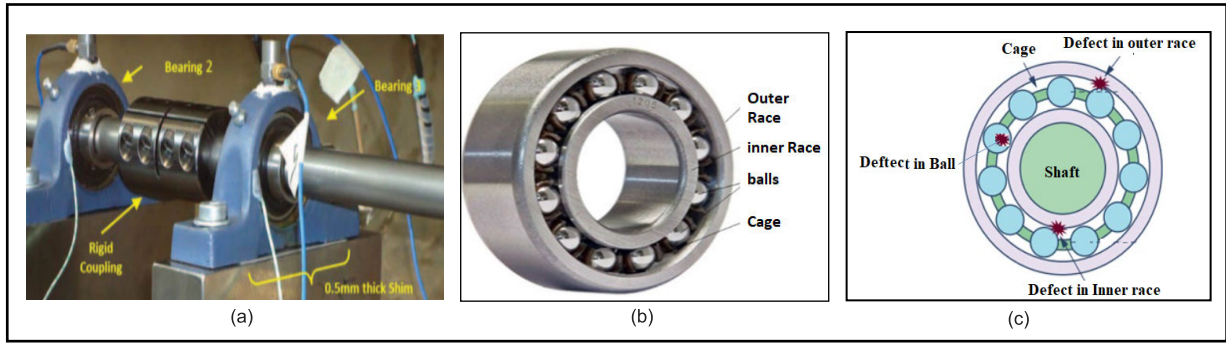


FIGURE 8. Bearing system [42].

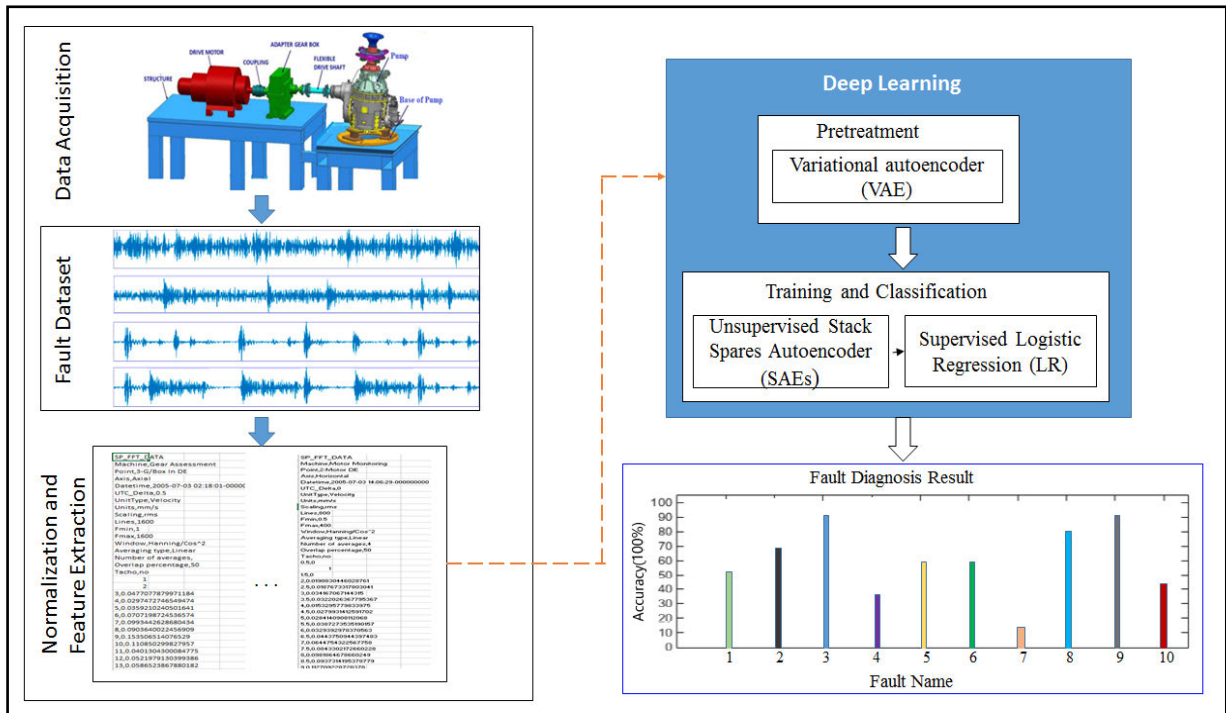


FIGURE 9. Architecture of the proposed model.

the number of extracted features, we need a method to improve the quality of the extracted signals by splitting them into several segments. Due to the variety of faults and the inadequacy of samples for each fault, the signals must be segmented and supplemented in order to extract as many features as possible in this work.

C. DATA AUGMENTATION USING VARIATIONAL AUTOENCODER

Once the features are extracted, we apply the Variational Autoencoder to generate and select more features by a forwarding selection process (making combinations from different features to obtain the best performance). In fact, during training the of the VAE, if two features are considered individually as input and the result is poor performance, then combining these two features together will lead to better results. This is referred as data augmentation.

The quality and quantity of training samples influence the efficiency of a deep learning model. Simulating data for vibrational signals using traditional methods usually requires effort and extra time, in the case of an unbalanced dataset or limited availability of fault samples or even both situations and could lead to complexity. However, when considering deep learning as a solution, the variational autoencoder can be used to accomplish data augmentation. Precisely, the decoder part, with its ability to recover the original data, can be used to generate pseudo-samples for the training and act as a good initialization for other deep learning models. Fig. 11 represents a sample for different data augmentation techniques.

The variational autoencoder (VAE) is a type of autoencoder that transforms input into latent variables and generates samples using a Gaussian distribution [44]. Fig. 12 depicts the architecture of the VAE. It assumes that a sample, A, must be produced from an input sample, B, using the distribution $p(B)$

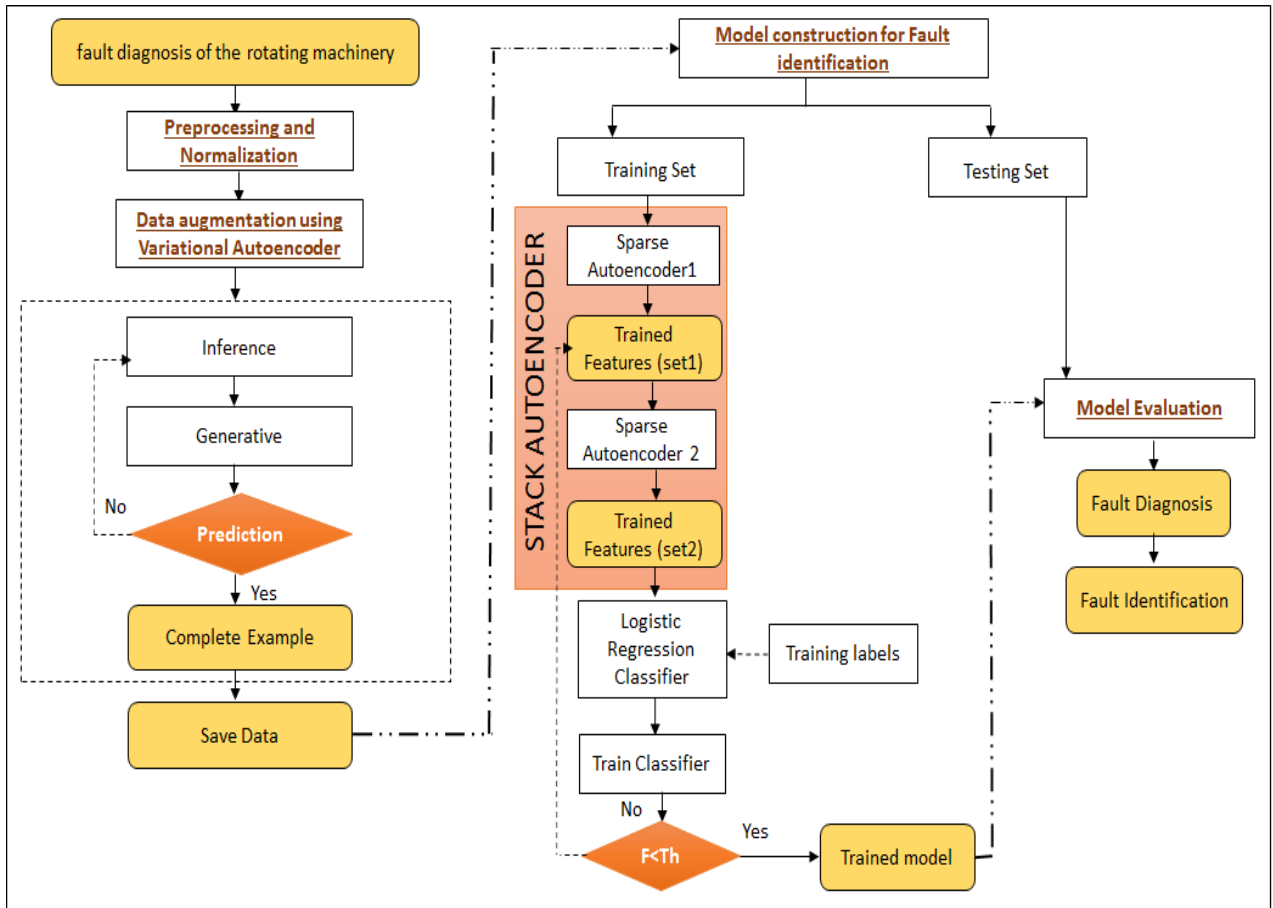


FIGURE 10. Flowchart of the proposed model.

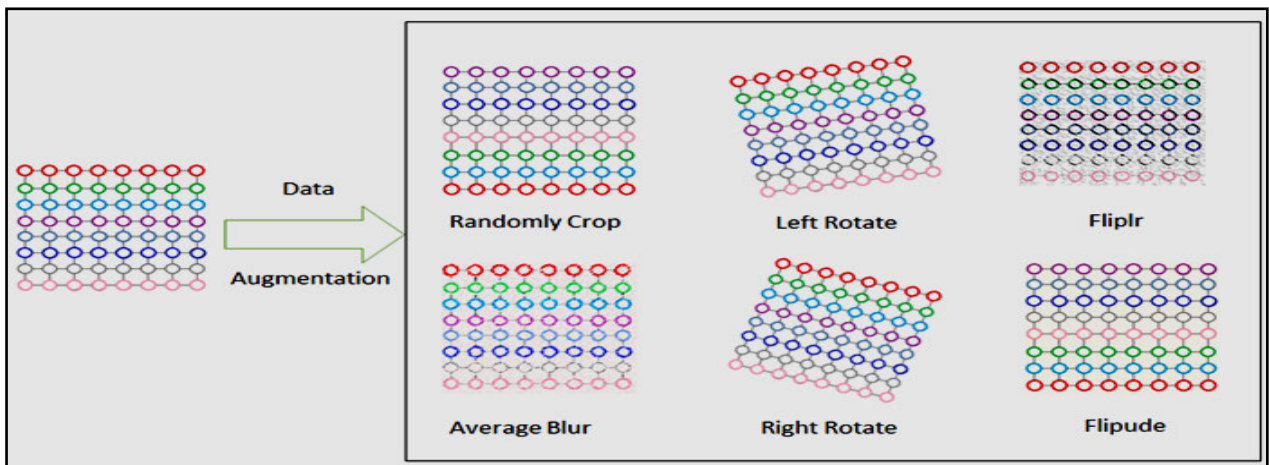


FIGURE 11. The data augmentation process of a two-dimensional feature map of a vibration signal.

(basically a Gaussian distribution $N(0, I)$ as a starting point. A is then obtained using the conditional distribution $p_{\theta}(A|B)$, where θ represents the decoder parameters. In contrast to standard autoencoders, Kingma *et al.* [14] proposed approximating the true posterior $p_{\theta}(B|A)$ by using the encoder

to parameterize the mean μ and the standard deviation, σ , of a diagonal Gaussian matrix $q_{\phi}(B|A)$ (where ϕ denotes the parameters of the encoder).

In this way, samples can be generated by decoding the sampling points in the Gaussian latent space $N(\mu, \text{diag}(\sigma^2))$.

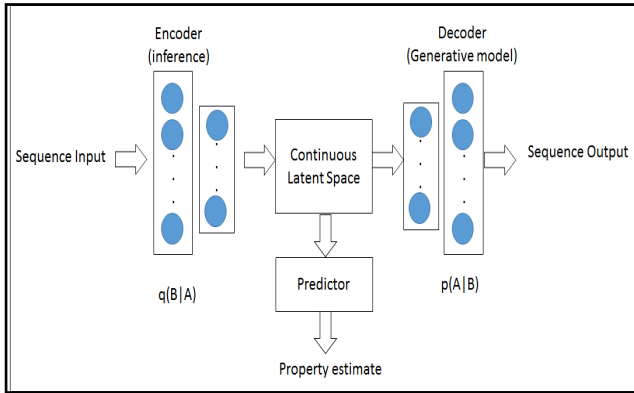


FIGURE 12. VAE architecture.

Usually, the lower the difference is between $q\varphi(B|A)$ and $p\theta(B|A)$ (KL), the better the approximation of the samples. In fact, $p\theta(B|A)$ is unknown; hence, it cannot be approximated directly, but indirectly by the evidence lower bound (ELBO) function:

$$ELBO = \log p\theta(A) - KL(q\varphi(B|A) || p\theta(B|A)) \quad (1)$$

where $\log p\theta(A)$ is the log-likelihood on B. Since the first term is a constant, the second term is supposed to be reduced by maximizing ELBO. The acronym ELBO can also be written as:

$$ELBO = E_{q\varphi(B|A)}[\log p\theta(A|B)] - KL(q\varphi(B|A) || p(B)) \quad (2)$$

where $E_{q\varphi(B|A)}[\log p\theta(A|B)]$ is the expectation of the conditional log likelihood of B, and $-KL(q\varphi(B|A) || p(B))$ is the Kullback–Leibler divergence between $q\varphi(B|A)$ and $p(B)$, which indicates that VAE assumes consistency between the learnable posterior and the prior $p(B)$. However, sampling from $N(\mu, \text{diag}(\sigma^2))$, produced difficulty in end-to-end training. Fortunately, in literature [45] it was replaced by $\mu + N(0, I) \times \sigma$.

D. MODEL CONSTRUCTION FOR FAULT IDENTIFICATION

The basic autoencoder [18], [26] is a symmetric architecture with at least three layers (input layer, hidden layer, and output layer), where the model is converted to a deep characteristic by adding more hidden layers. A simple explanation of its behavior is that the input layer encodes what it receives to a hidden representation and this is decoded again at the output layer to generate the input information. If this architecture is implemented successfully, then the optimal input features are obtained in the form of hidden weights with a minimum error. A variety of architectures and error minimization schemes have proposed different names and categories of autoencoder, as well as specifying their different functions. Fig. 13 details graphically the proposed architecture that contains two unsupervised SAEs, followed by a LR layer for classification.

The sparse autoencoder (SAE) [46] is a category of AE that limits the expression of hidden layer data with certain

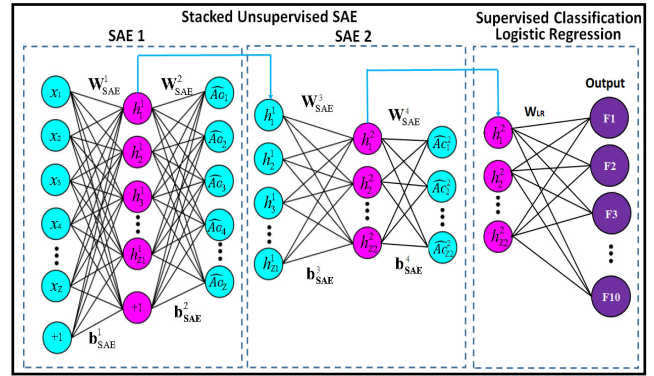


FIGURE 13. SAEs architecture.

constraints, to force the network to generate the output using a low dimensional expression while keeping the most discriminative features. Additionally, SAE adds a sparse penalty term to the objective function of the hidden layer during a concise expression generation. Accordingly, when a specific node value is close to 1, it is in an active state; otherwise, it is in an inactive state. In fact, the SAE requires inactive hidden nodes more than active ones. This is in turn forces fewer nodes to provide the output and requires a greater number of nodes in the hidden layer than in the input layer. Assume that the input data vector Ao and size is Z ; then the average output value \widehat{Ao}_j of the hidden layer node (j) is as follows:

$$\widehat{Ao}_j = \frac{1}{Z} \sum_{i=1}^Z [a_{hj}^2(x^i)] \quad (3)$$

where $a_{(hj)}^2(x^i)$ is the active unit corresponding to $h_j \cdot a = f_a(WX + b)$, W is the weight matrix, f_a is the activation function and b is the vector offset. KL represents the sparse penalty that consists of two Bernoulli distributions.

$$\sum_{j=1}^n KL(Ao, \widehat{Ao}_j) = \sum_{j=1}^n Ao \log \frac{Ao}{\widehat{Ao}_j} + (1 - Ao) \log \frac{1 - Ao}{1 - \widehat{Ao}_j} \quad (4)$$

If \widehat{Ao}_j is very close to Ao , KL is almost equal to zero and the average value of the hidden layer is zero as well; otherwise, KL increases rapidly. The square value and mean value of errors for the full samples are presented in equation 5. The mean value is used to limit the weight towards reduction in values (minimization). In addition, the objective functions add a sparse penalty term, as in equation 6. ϑ is the weight decay parameter, nk is the layer number of the network, sk denotes the neuron number in layer k , and W_{ji} is the connecting weight between neuron k in layer $k + 1$

$$h_{w,b} = \frac{1}{2} \|Ao^i - \widehat{Ao}_i\|^2 \quad (5)$$

$$J(W, b) = \left[\frac{1}{Z} \sum_{i=1}^Z (h_{w,b}) \right] + \frac{\vartheta}{2} \sum_k^{nk-1} \sum_{i=1}^{sk} \sum_{j=1}^{sk+1} (w_{ji}^k)^2 \quad (6)$$

$$J_{sparse}(w, b) = J(w, b) + \delta \sum_{j=1}^{S2} KL(A_o - \widehat{A_o}) \quad (7)$$

where δ is a sparse penalty term weight. Optimization of the minimum value of the objective function is reached using the back propagation algorithm and the gradient descent during training, and the final weights are then updated. The sparse penalty term is dependent on multiple factors. Using SAE for dimension reduction and reaching the most important features, a lower sparsity value is preferred.

The stacked sparse autoencoder (SSAE) [14] benefits from multiple hidden layers to extract features, layer by layer, where each hidden layer extracts features from a different perspective and dimensions. This qualifies the model for more generalization and enhances its capabilities.

The output features (that were learned using only unlabeled data) of the highest layer are investigated through the classification process by augmenting a Logistic Regression classifier after the high-level feature representations of input data are extracted through the first SAE (such as the Softmax regression classifier, as shown in equation 7) above the stacked sparse autoencoder's last hidden layer to fine-tune the deep learning architecture and boost learned features (using labeled data) in a supervised manner. To minimize the training error on the labeled training samples, the fine-tuning enforces gradient descent from the current setting of the parameters (i.e., labeled data may be used to change the weights, allowing changes to the features extracted by the layer of hidden units). Softmax regression, in this sense, is an extended form of LR that can be used for multiclass classification; it confirms that the activation of each output unit amounts to one, and the output can be thought of as a collection of conditional probabilities.

$$P(Y = i | R, W, b) = \frac{e^{w_i R + b_i}}{\sum_j e^{w_j R + b_j}} \quad (8)$$

where R is the performance of the stacked sparse autoencoder's last hidden layer, and W and b are the LR layer's weights and biases. The deep learning system is also fine-tuned [47] by taking into account very low learning rates on the preceding autoencoder layers.

E. MODEL EVALUATION

To evaluate the performance of the constructed model, we used different measures:

$$Precision = \frac{TP}{TP + FP} \quad (9)$$

$$Sensitivity = \frac{TP}{TP + FN} \quad (10)$$

$$Specificity = \frac{TN}{TP + FN} \quad (11)$$

$$F1 - score = \frac{Precision \times Sensitivity}{Precision + Sensitivity} \quad (12)$$

$$Accuracy = \frac{TN + TP}{TP + FP + TN + FN} \quad (13)$$

where TP (True Positive) denotes the number of positive samples correctly predicted as positive, and FP (False Positive) denotes the number of negative samples incorrectly predicted as positive; TN (True Negatives) and FN (False Negatives) denote the negative type, respectively. In this case, sensitivity refers to how well the model detects events in the positive class, while specificity refers to how accurate the positive class assignment is. Finally, the harmonic mean of sensitivity and precision is the F-measure. After data augmentation, Table 2 summarizes the number of samples for each fault class.

TABLE 2. Number of training and testing samples.

No.	Class Name	Number of samples for Training	Number of samples for Testing	Total number of samples
1	Bearing	117	50	167
2	Misalignment	175	75	250
3	Gear Assessment	161	69	230
4	Balancing	132	56	188
5	Mech Looseness	114	48	162
6	Motor Monitoring	142	60	202
7	Oil Whirl	112	48	160
8	Resonance	126	54	180
9	Soft Foot	137	58	195
10	Struct Looseness	168	72	240
Total		1384	590	1974

V. COMPUTATIONAL EXPERIMENTS AND DISCUSSION

The effects of VAE and SAE parameters are discussed in this section, followed by the results of the proposed classifier models. In order to verify the proposed method's detection efficiency, the experiments are divided into two sections: (1) checking the proposed method's parameters, and (2) comparing it to three standard learning methods (LR, RF, and NN), as well as three deep learning methods (autoencoder, CNN and DNN).

- Logistic Regression (LR): this is used as a neural network without a hidden layer and includes only two layers (input and output).
- Random Forest (RF): this is a multiple classifications method for dividing the dataset into several overlapping subsets. RF is produced by training various Decision Trees [44] with overlapping subsets of the initial set. During the testing stage, using all the trained trees, the input test sample is classified, and the final output is created based on the voting of the output from all the trees.
- Neuron Network (NN): this contains three layers (1 hidden layer, 1 input and 1 output).
- Basic Autoencoder
- CNN: stands for convolutional neural network, and it is a type of neural network used in computer vision. Convolutional layers completely linked layers, pooling

layers, and normalization layers are among the hidden layers. As a result, pooling and convolution functions are used activation functions rather than using the normal activation functions [19].

- DNN: this is a neural network with several layers between the input layers and output layers. It maps input to output by finding the correct mathematical manipulation [22].

A. VAE EVALUATION

To evaluate the impact of data augmentation on the proposed system, we trained the proposed model using the original data in addition to the augmented data, separately.

TABLE 3. Comparison of the proposed system with and without data augmentation samples.

Compared measurements	without VAE			With VAE		
	LR	RF	NN	LR	RF	NN
Precision	0.64	0.6	0.61	0.85	0.79	0.8
Accuracy	0.64	0.6	0.61	0.85	0.79	0.8
F1-Score	0.64	0.6	0.61	0.85	0.79	0.8
Sensitivity	0.644	0.603	0.62	0.856	0.794	0.801
Specificity	0.648	0.606	0.6	0.86	0.797	0.806

Table 3 summarizes the comparison of the proposed model with and without VAE, using three traditional techniques for classification. Without VAE, we noticed that the LR gave the best results comparing to RF and NN.

When we used the VAE, the LR showed higher results compared to the other methods for each case with or without the use of VAE.

Additionally, for more validation of the efficiency of the VAE in data augmentation, we compared it with five different methods used in the literature for data augmentation. These are briefly described below:

- Re-Sampling [48]: this is the straightforward technique to solve the class skew problem in tabular data. Here, we either under-sample or over-sample the available data to meet the requirement of equal class distribution.
- Noise addition [49]: this is a fundamental tool for data augmentation. Its main idea is based on adding different noises to data and hence generating more samples from the original sample.
- Sliding Window [50]: this model is mainly based on sliding a window of a specified size over the sample and applying some modification while sliding to produce different samples.
- Fourier transformation [51]: this is a popular method for augmenting signals. It is focused on imbalanced datasets in transitional sleep stages.
- GAN [52]: Data from a source domain is generalized to generate other within-class data objects using Generative Adversarial Networks. This generative process can be extended to novel, previously unknown classes of data since it is not based on the classes themselves.

A comparison of the results of these methods can be found in Fig. 14. We conclude that the highest accuracy can be achieved by using the deep learning methods GAN (0.82) and VAE (0.86). This result provides the effect of deep learning on the data augmentation process, which helps in reducing overfitting. Other methods also achieved a significant level of accuracy, including Noise Addition (0.79) and Sliding Window (0.78).

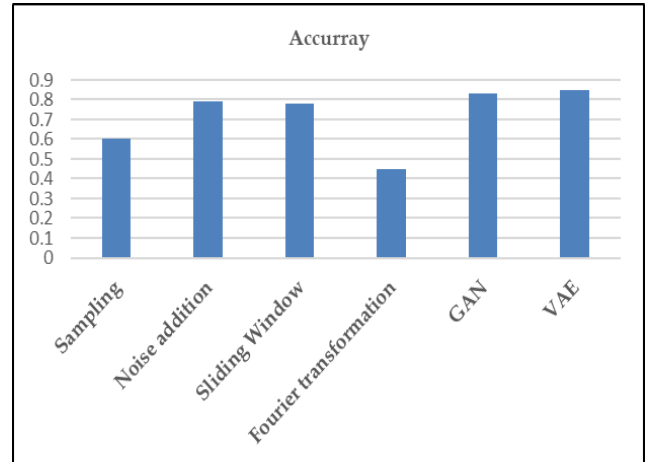


FIGURE 14. Accuracy of different data augmentation methods.

VAE and GAN are very similar techniques because they are two generative models. We applied those techniques using the proposed dataset to compare them and check their complexity and accuracy as well. Table 7 summaries the obtained results, where the training time represents the run time obtained for each iteration in the training process, and testing time refers to the data time during the test of one sample.

As shown in Table 7, VAE is faster to run and test than the other techniques. GAN and tnGAN are expensive, since they need a long time for training. Regarding testing time, values are in the same range (0.09 to 0.12). Therefore, the testing cost is the same for all the generative models. Regarding the accuracy, although all the techniques produced very close results, the VAE achieved the best result (0.86) comparing to the other techniques (GAN and tnGAN).

B. SAE EVALUATION

In this section, we first developed one SAE for feature extraction and then we investigated if adding one more SAE will enhance performance and then we added a third SAE. Table 4 presents the results obtained for each SAE. In fact, when we used only one SAE, the precision, accuracy and F1-score showed identical values of 0.87. When we added a second SAE, the values of these measures were enhanced to 0.93, but when we added the third SAE, the performance of the model was disrupted and decreased to 0.9. Therefore, the proposed architecture in Fig. 10 is proposed for obtaining better optimal results. Adding a third SAE also enhances the results, but with a tiny change that is inappropriate to training time and complexity as shown in Table 4.

TABLE 4. SAE evaluation.

Compared measurements	Stack SAE		
	1 SAE	2 SAEs	3 SAEs
Precision	0.87	0.93	0.932
Accuracy	0.87	0.93	0.933
F1-Score	0.87	0.93	0.931
Sensitivity	0.875	0.933	0.902
Specificity	0.88	0.936	0.904

TABLE 5. Evaluation of the classification method.

Compared measurements	VAE + Traditional Machine learning			The proposed deep learning architecture (2 SAEs)		
	LR	RF	NN	LR	RF	NN
Precision	0.85	0.79	0.8	0.93	0.84	0.87
Accuracy	0.85	0.79	0.8	0.932	0.84	0.87
F1-Score	0.85	0.79	0.8	0.93	0.84	0.87
Sensitivity	0.856	0.794	0.801	0.933	0.841	0.873
Specificity	0.86	0.797	0.806	0.936	0.844	0.877

In the second step, we evaluated the proposed framework by integrating three methods for classification. Here, we proposed two sets of experiences, as shown in Table 5; the first set was to classify the samples directly after data augmentation without using the stacked SAE and the second set was conducted to establish the importance of using SAE before classification to enhance the classification performance. When classification was applied without using a stacked SAE, by applying one of the three traditional methods (LR, RF and NN) defined previously in section five, we noticed that LR gave better results than the other techniques. Therefore, a simple neural network without any hidden layer is enough to obtain good results. The accuracy of the neural network with one hidden layer (NN) was very similar to that of the LR (accuracy = 0.8 for NN, 0.85 for LR); thus, one hidden layer is insufficient to obtain the best performance. In other words, an overly large number of neurons in the hidden layers can increase the time required to train the network to the point that adequate training is impossible. Deep learning can help to improve the situation and improve classification efficiency.

As shown in the second part of Table 5, using SAE showed an excellent result when it was added to one of the three classifiers, such as LR, where the accuracy, precision, and F1-score achieved were 0.932, 0.93 and 0.93, respectively.

C. CROSS VALIDATION WITH DIFFERENT DEEP LEARNING APPROACHES

In this stage, we compared the proposed framework with other deep learning techniques (Basic autoencoder, CNN and DNN). Table 6 shows the comparison between these techniques and the proposed framework, which combines two types of autoencoders (VAE and stacked SAE with RL) using the same dataset. The classification time is just the time between the fully connected layer and the output layer and

TABLE 6. Cross validation of the proposed architecture versus state-of-the-art deep learning approaches.

Compared measurements	Our proposed framework	Basic autoencoder	CNN	DNN
Classification time(s)	0.06	0.04	0.07	0.07
Correct classes	10	8	9	10
Incorrect classes	0	1	1	0
Error rate	0.01	0.2	0.1	0.06
Accuracy	0.932	0.83	0.88	0.9

TABLE 7. The obtained results after applying VAE and GAN techniques using the proposed dataset.

Methods	Accuracy	Training time (s)	Testing time (s)
VAE	0.86	1.01	0.09
GAN [52]	0.82	1.2	0.1
tnGAN [28]	0.84	1.8	0.12

does not include the training time. With the basic autoencoder, the classification is very fast, but the error rate is higher compared to the other methods, since it achieved a smaller number of correct classes compared to the other methods. Regarding the accuracy, the basic autoencoder achieved the lowest value (0.83). Both CNN and DNN had the same classification time (0.07) but different error rates (0.1 for CNN and 0.06 for DNN), because DNN achieves better accuracy than CNN. Regarding the proposed model, it is faster than CNN and DNN and slower than the basic autoencoder because it contains more neurons. With our framework, we classified all the signals with an error rate equals to 0.01 and an accuracy equal to 0.932. This result is very important, since it supports the efficiency of the proposed techniques used in constructing our framework.

VI. CONCLUSION

In this paper, we have presented a new deep architecture based on stacked variant autoencoders for multi-fault machinery identification with imbalanced samples. The proposed model begins with the data augmentation process, which was employed using a Variational Autoencoder for increasing the initial data samples from an imbalanced dataset with small size using Gaussian distribution. The obtained preprocessed vibration signals were then injected into a deep architecture containing two consequent unsupervised sparse autoencoders with a penalty term that helps in acquiring more abstract and essential features as well as avoiding redundancy. The output of the second SAE was integrated on a supervised Logistic Regression with 10 classes to help in achieving accurate fault identification. Several experiments have shown that our framework can learn high-quality discriminative features and achieve better performance in signal classification, where the achieved accuracy of the proposed model is 93.2%.

ACKNOWLEDGMENT

This research project was funded by the Deanship of Scientific Research, Princess Nourah bint Abdulrahman University, through the Program of Research Project Funding After Publication, Grant No. (41-PRFA-P-38).

REFERENCES

- [1] C.-C. Wang, Y. Kang, P.-C. Shen, Y.-P. Chang, and Y.-L. Chung, "Applications of fault diagnosis in rotating machinery by using time series analysis with neural network," *Expert Syst. Appl.*, vol. 37, no. 2, pp. 1696–1702, Mar. 2010.
- [2] J.-D. Wu and J.-J. Chan, "Faulted gear identification of a rotating machinery based on wavelet transform and artificial neural network," *Expert Syst. Appl.*, vol. 36, no. 5, pp. 8862–8875, Jul. 2009.
- [3] V. Sugumaran and K. I. Ramachandran, "Effect of number of features on classification of roller bearing faults using SVM and PSVM," *Expert Syst. Appl.*, vol. 38, no. 4, pp. 4088–4096, 2011.
- [4] Y. Zhang, H. Zuo, and F. Bai, "Classification of fault location and performance degradation of a roller bearing," *Measurement*, vol. 46, no. 3, pp. 1178–1189, 2013.
- [5] C. Y. Yang and T. Y. Wu, "Diagnostics of gear deterioration using EEMD approach and PCA process," *Measurement*, vol. 61, pp. 75–87, Feb. 2015.
- [6] X. Xue, J. Zhou, Y. Xu, W. Zhu, and C. Li, "An adaptively fast ensemble empirical mode decomposition method and its applications to rolling element bearing fault diagnosis," *Mech. Syst. Signal Process.*, vol. 62, pp. 444–459, Oct. 2015.
- [7] A. R. Ramos, J. M. B. de Lázaro, A. J. da Silva Neto, C. C. Corona, J. L. Verdegay, and O. Llanes-Santiago, "An approach to fault diagnosis using fuzzy clustering techniques," in *Advances in Intelligent Systems and Computing*, vol. 643, J. Kacprzyk, E. Szmidt, S. Zadrozny, K. Atanassov and M. Krawczak, Eds. Cham, Switzerland: Springer, 2017, pp. 232–243, doi: 10.1007/978-3-319-66827-7_21.
- [8] M. Zair, C. Rahmoune, and D. Benazzouz, "Multi-fault diagnosis of rolling bearing using fuzzy entropy of empirical mode decomposition, principal component analysis, and SOM neural network," *Proc. Instit. Mech. Eng. C, J. Mech. Eng. Sci.*, vol. 233, pp. 3317–3328, May 2019.
- [9] M. Cerrada, R. Sanchez, D. Cabrera, G. Zurita, and C. Li, "Multi-stage feature selection by using genetic algorithms for fault diagnosis in gearboxes based on vibration signal," *Sensors*, vol. 15, pp. 23903–23926, 2015.
- [10] L. Pan, D. Zhu, S. She, A. Song, X. Shi, and S. Duan, "Gear fault diagnosis method based on wavelet-packet independent component analysis and support vector machine with kernel function fusion," *Adv. Mech. Eng.*, vol. 10, no. 11, 2018, Art. no. 1687814018811036.
- [11] H. Mekki, A. Melit, and H. Salhi, "Artificial neural network-based modeling and fault detection of partial shaded photovoltaic modules," *Simul. Modell. Pract. Theory*, vol. 67, pp. 1–13, Sep. 2016.
- [12] X. Zhu, D. Hou, P. Zhou, Z. Han, Y. Yuan, W. Zhou, and Q. Yin, "Rotor fault diagnosis using a convolutional neural network with symmetrized dot pattern images," *Measurement*, vol. 138, pp. 526–535, May 2019.
- [13] Z. Guan, X. Liao, K. Li, and P. Chen, "A precise diagnosis method of structural faults of rotating machinery based on combination of empirical mode decomposition, sample entropy, and deep belief network," *Sensors*, vol. 19, no. 3, p. 591, Jan. 2019.
- [14] W. Du, J. Zhou, Z. Wang, R. Li, and J. Wang, "Application of improved singular spectrum decomposition method for composite fault diagnosis of gear boxes," *Sensors*, vol. 18, no. 11, p. 3804, Nov. 2018.
- [15] Z. Wang, J. Wang, and W. Du, "Research on fault diagnosis of gearbox with improved variational mode decomposition," *Sensors*, vol. 18, no. 10, p. 3510, Oct. 2018.
- [16] X. Chen, G. Cheng, H. Li, and Y. Li, "Research of planetary gear fault diagnosis based on multi-scale fractal box dimension of CEEMD and ELM," *Strojinski Vestnik J. Mech. Eng.*, vol. 63, no. 1, pp. 45–55, Jan. 2017.
- [17] X. Li, W. Zhang, and Q. Ding, "Cross-domain fault diagnosis of rolling element bearings using deep generative neural networks," *IEEE Trans. Ind. Electron.*, vol. 66, no. 7, pp. 5525–5534, Jul. 2019.
- [18] Z. Xiang, X. Zhang, W. Zhang, and X. Xia, "Fault diagnosis of rolling bearing under fluctuating speed and variable load based on TCO spectrum and stacking auto-encoder," *Measurement*, vol. 138, pp. 162–174, May 2019.
- [19] S. Guo, T. Yang, W. Gao, C. Zhang, and Y. Zhang, "An intelligent fault diagnosis method for bearings with variable rotating speed based on pythagorean spatial pyramid pooling CNN," *Sensors*, vol. 18, no. 11, p. 3857, Nov. 2018.
- [20] M. J. Hasan and J.-M. Kim, "Bearing fault diagnosis under variable rotational speeds using stockwell transform-based vibration imaging and transfer learning," *Appl. Sci.*, vol. 8, no. 12, p. 2357, Nov. 2018.
- [21] R. Huang, Y. Liao, S. Zhang, and W. Li, "Deep decoupling convolutional neural network for intelligent compound fault diagnosis," *IEEE Access*, vol. 7, pp. 1848–1858, 2019.
- [22] R. Zhang, Z. Peng, L. Wu, B. Yao, and Y. Guan, "Fault diagnosis from raw sensor data using deep neural networks considering temporal coherence," *Sensors*, vol. 17, no. 3, p. 549, Mar. 2017.
- [23] Y. Yang, P. Fu, and Y. He, "Bearing fault automatic classification based on deep learning," *IEEE Access*, vol. 6, pp. 71540–71554, 2018.
- [24] J. He, S. Yang, and C. Gan, "Unsupervised fault diagnosis of a gear transmission chain using a deep belief network," *Sensors*, vol. 17, no. 7, p. 1564, Jul. 2017.
- [25] G. Jiang, H. He, P. Xie, and Y. Tang, "Stacked multilevel-denoising autoencoders: A new representation learning approach for wind turbine gearbox fault diagnosis," *IEEE Trans. Instrum. Meas.*, vol. 66, no. 9, pp. 2391–2402, Sep. 2017.
- [26] G. Liu, H. Bao, and B. Han, "A stacked autoencoder-based deep neural network for achieving gearbox fault diagnosis," *Math. Problems Eng.*, vol. 2018, pp. 1–10, Jul. 2018, doi: 10.1155/2018/5105709.
- [27] H. Zhang, X. Hu, D. Ma, R. Wang, and X. Xie, "Insufficient data generative model for pipeline network leak detection using generative adversarial networks," *IEEE Trans. Cybern.*, early access, Dec. 9, 2020, doi: 10.1109/TCYB.2020.3035518.
- [28] X. Hu, H. Zhang, D. Ma, and R. Wang, "A tGAN-based leak detection method for pipeline network considering incomplete sensor data," *IEEE Trans. Instrum. Meas.*, vol. 70, pp. 1–10, 2021.
- [29] H. Shao, M. Xia, J. Wan, and C. De Silva, "Modified stacked auto-encoder using adaptive Morlet wavelet for intelligent fault diagnosis of rotating machinery," *IEEE/ASME Trans. Mechatronics*, early access, Feb. 9, 2021, doi: 10.1109/TMECH.2021.3058061.
- [30] Z. He, H. Shao, P. Wang, J. Lin, J. Cheng, and Y. Yang, "Deep transfer multi-wavelet auto-encoder for intelligent fault diagnosis of gearbox with few target training samples," *Knowl.-Based Syst.*, vol. 191, Mar. 2020, Art. no. 105313, doi: 10.1016/j.knsys.2019.105313.
- [31] J. M. McCarthy and G. S. Soh, *Geometric Design of Linkages*. New York, NY, USA: Springer, 2010.
- [32] K. Kinbara and T. Aida, "Toward intelligent molecular machines: Directed motions of biological and artificial molecules and assemblies," *Chem. Rev.*, vol. 105, no. 4, pp. 1377–1400, Apr. 2005, doi: 10.1021/cr030071r.
- [33] M. Guarnieri, "Electricity in the age of enlightenment [historical]," *IEEE Ind. Electron. Mag.*, vol. 8, no. 3, pp. 60–63, Sep. 2014, doi: 10.1109/MIE.2014.2335431.
- [34] A. Glowacz and W. Glowacz, "Vibration-based fault diagnosis of commutator motor," *Shock Vib.*, vol. 2018, pp. 1–10, Oct. 2018, doi: 10.1155/2018/7460419.
- [35] M. Nakhaeinejad and S. Ganeriwala, "Observations on dynamic response of misalignments," SpectraQuest Inc., Richmond, VA, USA, Tech. Rep., 2009.
- [36] A. Sommer, J. Meagher, and X. Wu, "Gear defect modeling of a multiple-stage gear train," *Model. Simul. Eng.*, vol. 2011, pp. 1–8, Jan. 2011, doi: 10.1155/2011/754257.
- [37] M. A. Saleem, G. Diwakar, and M. R. S. Satyanarayana, "Detection of unbalance in rotating machines using shaft deflection measurement during its operation," *IOSR J. Mech. Civil Eng.*, vol. 3, no. 3, pp. 8–20, 2012, doi: 10.9790/1684-0330820.
- [38] W. Fiebig and J. Wrobel, "Use of mechanical resonance in impact machines," *MATEC Web Conf.*, vol. 211, Oct. 2018, Art. no. 17006, doi: 10.1051/mateconf/201821117006.
- [39] L. Ma, M. Sanada, S. Morimoto, and Y. Takeda, "Prediction of iron loss in rotating machines with rotational loss included," *IEEE Trans. Magn.*, vol. 39, no. 4, pp. 2036–2041, Jul. 2003, doi: 10.1109/TMAG.2003.812706.
- [40] W. X. Lu and F. L. Chu, "Experimental investigation of pedestal looseness in a rotor-bearing system," *Key Eng. Mater.*, vols. 413–414, pp. 599–605, Jun. 2009, doi: 10.4028/www.scientific.net/KEM.413-414.599.
- [41] F. Elasha, C. Ruiz-Carcel, D. Mba, V. H. Jaramillo, and J. R. Ottewill, "Detection of machine soft foot with vibration analysis," *Insight Non-Destructive Test. Condition Monitor.*, vol. 56, no. 11, pp. 622–626, Nov. 2014, doi: 10.1784/insi.2014.56.11.622.
- [42] N. Azeez and A. C. Alex, "Detection of rolling element bearing defects by vibration signature analysis: A review," in *Proc. Int. Conf. Magn., Mach. Drives (AICERA/CMMD)*, Kottayam, India, 2014, pp. 1–5, doi: 10.1109/AICERA.2014.6908270.

- [43] A. El-Shafei, S. H. Tawfick, M. S. Raafat, and G. M. Aziz, "Some experiments on oil whirl and oil whip," *J. Eng. Gas Turbines Power*, vol. 129, no. 1, pp. 144–153, Jan. 2007, doi: [10.1115/1.2181185](https://doi.org/10.1115/1.2181185).
- [44] Y. Pu, Z. Gan, R. Henao, X. Yuan, C. Li, A. Stevens, and L. Carin, "Variational autoencoder for deep? Learning of images, labels and captions," in *Proc. 29th Conf. Neural Inf. Process. Syst. (NIPS)*, Barcelona, Spain, 2016, pp. 2352–2360.
- [45] C. Che, H. Wang, Q. Fu, and X. Ni, "Combining multiple deep learning algorithms for prognostic and health management of aircraft," *Aerosp. Sci. Technol.*, vol. 94, Nov. 2019, Art. no. 105423, doi: [10.1016/j.ast.2019.105423](https://doi.org/10.1016/j.ast.2019.105423).
- [46] M. Sohaib and J.-M. Kim, "Reliable fault diagnosis of rotary machine bearings using a stacked sparse autoencoder-based deep neural network," *Shock Vib.*, vol. 2018, pp. 1–11, May 2018, doi: [10.1155/2018/2919637](https://doi.org/10.1155/2018/2919637).
- [47] Y. Chen, Z. Lin, X. Zhao, G. Wang, and Y. Gu, "Deep learning-based classification of hyperspectral data," *IEEE J. Sel. Topics Appl. Earth Observ. Remote Sens.*, vol. 7, no. 6, pp. 2094–2107, Jun. 2014, doi: [10.1109/JSTARS.2014.2329330](https://doi.org/10.1109/JSTARS.2014.2329330).
- [48] A. G. Nath, A. Sharma, S. S. Udmale, and S. K. Singh, "An early classification approach for improving structural rotor fault diagnosis," *IEEE Trans. Instrum. Meas.*, vol. 70, pp. 1–13, 2021, doi: [10.1109/TIM.2020.3043959](https://doi.org/10.1109/TIM.2020.3043959).
- [49] N. Sun, X. Mo, T. Wei, D. Zhang, and W. Luo, "The effectiveness of noise in data augmentation for fine-grained image classification," in *Pattern Recognition (Lecture Notes in Computer Science)*, vol. 12046, S. Palaihnakote G. S. di Baja, L. Wang and W. Yan, Eds. Cham, Switzerland: Springer, 2020, pp. 779–792, doi: [10.1007/978-3-030-41404-7_55](https://doi.org/10.1007/978-3-030-41404-7_55).
- [50] A. Helwan and D. U. Ozsahin, "Sliding window based machine learning system for the left ventricle localization in MR cardiac images," *Appl. Comput. Intell. Soft Comput.*, vol. 2017, pp. 1–9, Jan. 2017, doi: [10.1155/2017/3048181](https://doi.org/10.1155/2017/3048181).
- [51] E. Lashgari, D. Liang, and U. Maoz, "Data augmentation for deep-learning-based electroencephalography," *J. Neurosci. Methods*, vol. 346, Jul. 2020, Art. no. 108885, doi: [10.1016/j.jneumeth.2020.108885](https://doi.org/10.1016/j.jneumeth.2020.108885).
- [52] A. Antoniou, A. Storkey, and H. Edwards, "Data augmentation generative adversarial networks," 2017, *arXiv:1711.04340*. [Online]. Available: <http://arxiv.org/abs/1711.04340>



HANEN KARAMTI received the bachelor's and master's degrees in computer science and multimedia from the High Institute of Computer Science and Multimedia of Sfax (ISIMS), University of Sfax, Tunisia, and the Ph.D. degree in computer science from the National Engineering School of Sfax, University of Sfax, in cooperation with the University of La Rochelle, France, and the University of Hanoi, Vietnam. She is currently an Assistant Professor with Princess Norah bint Abdulrahman University, Riyadh, Saudi Arabia. Her research interests include information retrieval, multimedia systems, image retrieval, health informatics, big data, and data analytics.

MAHA M. A. LASHIN received the Ph.D. degree in artificial intelligent from Cairo University, Egypt. She is currently an Associate Professor in mechanical design and production with the College of Engineering, Princess Nourah bint Abdulrahman University (PNU), Saudi Arabia, and a Supervisor of master's and philosophy doctor degrees for students of engineering colleges, such as smart memory alloy development for the effective use of control systems, diagnosis of machinery malfunctions by analyzing the vibrations using genetic algorithms, modeling and simulation of the static and dynamic performance of sandwich beams, automated monitoring and measuring improvement of production system performance, and control of air handling unit as a method of reducing power consuming. She has published more than 30 articles in international journals in fields of automatic control, mechanical vibration analysis, artificial intelligence, and composite materials.

FADWA M. ALROWAIS received the B.Sc. degree (Hons.) in computer and information sciences with a focus on computer applications and the M.Sc. degree in computer science from the College of Computer and Information Sciences, King Saud University, Saudi Arabia, in 1996 and 2005, respectively, and the Ph.D. degree in computer science from the Faculty of Electronics and Computer Sciences, Southampton University, U.K., in 2016. She has 24 years academic experience, as she has worked with the College of Computer and Information Sciences and the College of Engineering, Princess Nourah bint Abdulrahman University.



ABEER M. MAHMOUD received the B.Sc. and M.Sc. degrees in computer science from Ain Shams University, Egypt, in 2000 and 2004, respectively, and the Ph.D. degree in computer science from Niigata University, Japan, in 2010. She was an Assistant Lecturer, an Assistant Professor, and an Associate Professor with the Faculty of Computer and Information Sciences, Ain Shams University. Her research interests include artificial intelligence, medical data mining, machine learning, big data, and robotic simulation systems.

• • •